Inhibition of cyclin-dependent kinases, GSK-3β and CK1 by hymenialdisine, a marine sponge constituent

L Meijer[1], A-MWH Thunnissen[2*], AW White[3], M Garnier[1], M Nikolic[4†], L-H Tsai[4], J Walter[5], KE Cleverley[6], PC Salinas[6], Y-Z Wu[7], J Biernat[7], E-M Mandelkow[7], S-H Kim[2] and GR Pettit[3]

Background: Over 2000 protein kinases regulate cellular functions. Screening for inhibitors of some of these kinases has already yielded some potent and selective compounds with promising potential for the treatment of human diseases.

Results: The marine sponge constituent hymenialdisine is a potent inhibitor of cyclin-dependent kinases, glycogen synthase kinase-3β and casein kinase 1. Hymenialdisine competes with ATP for binding to these kinases. A CDK2–hymenialdisine complex crystal structure shows that three hydrogen bonds link hymenialdisine to the Glu81 and Leu83 residues of CDK2, as observed with other inhibitors. Hymenialdisine inhibits CDK5/p35 *in vivo* as demonstrated by the lack of phosphorylation/down-regulation of Pak1 kinase in E18 rat cortical neurons, and also inhibits GSK-3 *in vivo* as shown by the inhibition of MAP-1B phosphorylation. Hymenialdisine also blocks the *in vivo* phosphorylation of the microtubule-binding protein tau at sites that are hyperphosphorylated by GSK-3 and CDK5/p35 in Alzheimer's disease (cross-reacting with Alzheimer's-specific AT100 antibodies).

Conclusions: The natural product hymenialdisine is a new kinase inhibitor with promising potential applications for treating neurodegenerative disorders.

Addresses: [1]CNRS, Station Biologique, BP 74, 29682 Roscoff cedex, Bretagne, France. [2]University of California, Department of Chemistry, Berkeley, CA, USA. [3]Arizona State University, Cancer Research Institute, Tempe, AZ, USA. [4]Howard Hughes Medical Institute, Department of Pathology, Harvard Medical School, 200 Longwood Avenue, Boston, MA, USA. [5]Department of Molecular Biology, Central Institute of Mental Health, 68159 Mannheim, Germany. [6]The Randall Institute, Developmental Biology Research Centre, King's College London, 26–29 Drury Lane, London WC2B 5RL, UK. [7]Max-Planck Unit for Structural Molecular Biology, Notkestrasse 85, D-22603 Hamburg, Germany.

Present addresses: *Laboratory of Biophysical Chemistry, University of Groningen, Nijenborgh 4, 9747 AG Groningen, The Netherlands. †Department of Experimental Pathology, GKT School of Medicine, King's College London, London, SE1 9RT, UK.

Correspondence: Laurent Meijer
E-mail: meijer@sb-roscoff.fr

Key words: Alzheimer's disease, cyclin-dependent kinases, glycogen synthase kinase, hymenialdisine, tau

Received: **4 August 1999**
Revisions requested: **14 September 1999**
Revisions received: **27 September 1999**
Accepted: **6 October 1999**

Published: **20 December 1999**
Publication delayed at the author's request

Chemistry & Biology 2000, **7**:51–63

1074-5521/00/$ – see front matter
© 2000 Elsevier Science Ltd. All rights reserved.

Introduction

Alzheimer's disease (AD) affects 5–10% of the population over 65 years of age. The dementia associated with AD results from the selective death of neurons, which is associated with several anatomo-pathological hallmarks such as senile neuritic plaques and neurofibrillary tangles. Three molecular actors clearly play a role in the development of AD: the amyloid β peptide (Aβ), presenilins-1 and -2 and the microtubule-associated protein tau. The senile neuritic plaques form an extracellular core of deposited amyloid β peptide, derived from proteolytic cleavage of the amyloid precursor protein (β-APP; reviewed in [1]). The neurofibrillary tangles are intracellular aggregates of paired helical filaments (PHFs) that consist mainly of hyperphosphorylated tau proteins. Hyperphosphorylation occurs on more than 20 sites and is carried out by two proline-directed kinases, glycogen synthase kinase-3β (GSK-3β) and cyclin-dependent kinase 5 (CDK5/p35) (reviewed in [2,3]), and possibly also by casein kinase 1 (CK1) [4]. Finally, mutations in the transmembrane proteins presenilin genes are the most common cause of early onset familial AD (reviewed in [1,5]).

The links between the three proteins, Aβ, presenilins and tau, have remained elusive until recently (reviewed in [5,6]). Presenilins appear to be unusual aspartyl proteases

Figure 1

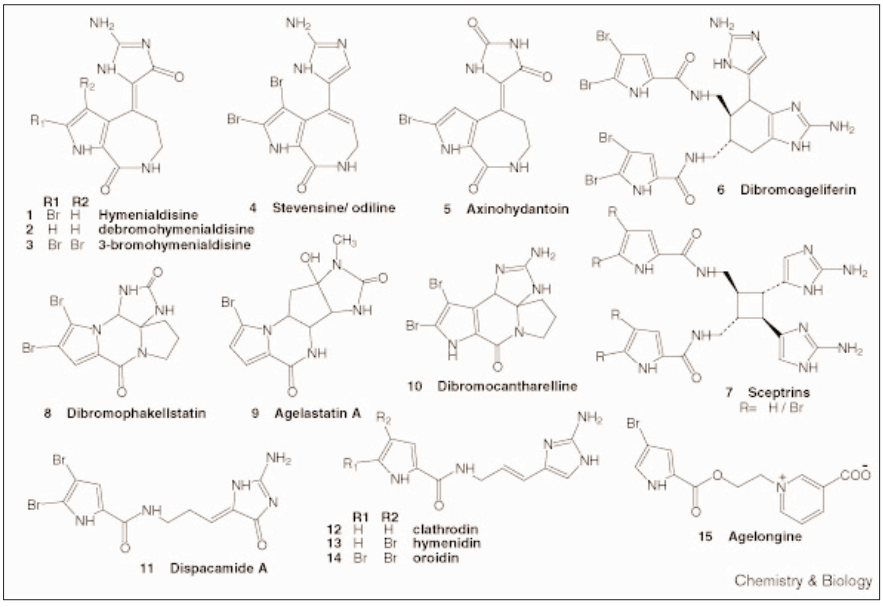

Structure of hymenialdisine and related metabolites isolated from marine sponges.

that activate themselves autocatalytically. They cleave β-APP to generate Aβ [7], particularly the most aggregation-prone and neurotoxic amyloid β peptide, $A\beta_{42}$. Presenilins also directly associate with β-catenin [8,9] and GSK-3β [10], two components of the Wnt signalling pathway. Activation of this pathway leads to inhibition of GSK-3β and results in β-catenin stabilisation. The level of β-catenin is indeed lower in extracts of brain with presenilin-1 mutations compared with controls or sporadic Alzheimer's cases [9]. Interestingly, expressed tau is phosphorylated in cells co-transfected with mutant presenilin-1 but not in cells expressing wild-type presenilin-1 [10]. Aβ treatment of cultured hippocampal neurons results in stimulation of GSK-3β activity [11]. All these results place tau hyperphosphorylation downstream of presenilins and Aβ action. Finally, the recent discovery of tau mutations in AD-related diseases (reviewed in [3]) and the recently described functions of tau in regulating intracellular traffic along microtubules [12] have renewed the interest in understanding the causal link between tau hyperphosphorylation and the pathways leading to the cellular modifications responsible for AD.

Because protein kinases play an essential role in virtually all cellular processes and in most diseases, extensive searches for selective inhibitors of these enzymes have been carried out (reviewed in [13]). Our laboratory has focused its efforts on the cyclin-dependent kinase (CDK) family. CDKs are involved in cell-cycle control (CDK1–4, 6 and 7), thymocyte apoptosis (CDK2), neuronal functions (CDK5) and transcriptional control (CDK7–9) (reviewed in [14–16]). In nervous tissues CDK5/p35 phosphorylates the microtubule-associated proteins tau and MAP-1B (reviewed in [2,17]), Pak1 kinase [18] and neurofilament subunits [19]. Intensive screening has identified a series of chemical CDK inhibitors (reviewed in [20–22]), such as olomoucine [23], roscovitine [24,25], purvalanol [26], flavopiridol [27], indirubins [28] and paullones [29,30]. Some of these compounds display remarkable selectivity and efficiency.

In this article we report the discovery of hymenialdisine (HD, **1**; Figure 1) as a very potent inhibitor of CDK1, CDK2 and CDK5, GSK-3β and CK1. HD has been isolated from several species of marine sponges along with a variety of related metabolites (Figure 1) [31]. We also report the crystal structure of a CDK2–HD complex, which provides an important advance in understanding the molecular mechanism of CDK inhibition. HD was found to inhibit the *in vivo* phosphorylation of specific neuronal proteins by GSK-3β and CDK5. In particular, the AD-characteristic phosphorylation of tau is completely inhibited by HD *in vivo*. As a potent and rather selective inhibitor of kinases involved in AD and other degenerative disorders, HD could be a lead compound for evaluating the importance of tau hyperphosphorylation in neurodegenerative diseases and for interfering with this molecular event.

Results

HD potently inhibits CDK1, CDK2, CDK5, GSK-3β and CK1

While screening compounds isolated from marine invertebrates and plants for new CDK inhibitors [32], we discovered HD (**1**) to be a potent inhibitor of CDK1/cyclin B (Figure 2, Table 1). HD belongs to a family of chemically and metabolically related, marine-sponge-derived natural products (which contain both bromopyrrole and

Figure 2

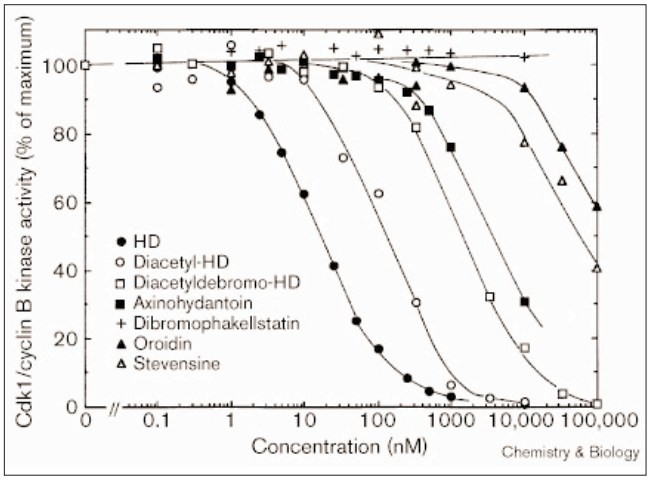

Inhibition of CDK1/cyclin B by HD analogues. CDK1/cyclin B was assayed as described in the Supplementary material section. Activity is presented as % of maximal activity (i.e. in the absence of inhibitors).

guanidine groups) [31,33–37]. In the presence of 15 μM ATP, HD was found to inhibit CDK1/cyclin B, CDK2/cyclin A, CDK2/cyclin E, CDK3/cyclin E and CDK5/p35 with IC_{50} values of 22, 70, 40, 100 and 28 nM, respectively (Table 1). As observed with olomoucine [23], roscovitine [24], indirubin-3′-monoxime [28], kenpaullone [29] and, in contrast to flavopiridol [38], HD had limited effect on CDK4/cyclin D1 and CDK6/cyclin D2 (IC_{50} values of 600 and 700 nM, respectively).

HD was next tested on a variety of highly purified kinases (IC_{50} values are shown in Table 1). Kinase activities were assayed with appropriate substrates and 15 μM ATP (this concentration was comparable to previously published studies) and in the presence of increasing concentrations of HD. Most kinases tested were poorly or not inhibited (IC_{50} > 1 μM). However, two kinases, GSK-3β and CK1, were strongly sensitive to HD (IC_{50} values of 10 and 35 nM, respectively; Figure 2, Table 1). The HD-sensitive kinases were also assayed *in vitro* with physiologically relevant substrates: a fragment of presenilin-2 [39] for CK1 (Figure 3), Pak1 [18] for CDK5/p35 (Figure 4), the insulin-receptor substrate IRS-1 [40] (data not shown) or tau for GSK-3β (Figure 5). The sensitivity of the kinases towards HD was comparable to the sensitivity of the same kinases assayed with more artificial substrates.

We next tested some natural HD-related compounds isolated from marine sponges and some synthetically modified HD analogues on CDK1/cyclin B, CDK5/p35, GSK-3β and CK1 (Figure 2; Table 2). HD was the most active compound. Interestingly, dibromocantharelline (**10**) displayed a significant inhibitory effect towards GSK-3β (IC_{50} = 3 μM). Hymenidin (**13**) was selective for CDK5.

Table 1

Kinase inhibition selectivity of hymenialdisine.

Enzyme	IC_{50} (nM)
CDK1/cyclin B	22
CDK2/cyclin A	70
CDK2/cyclin E	40
CDK3/cyclin E	100
CDK4/cyclin D1	600
CDK5/p25	28
CDK6/cyclin D2	700
Erk1	470
Erk2	2000
c-raf	>10,000
MAPKK	1200
c-Jun amino-terminal kinase	8500
Protein kinase C α	700
Protein kinase C β1	1200
Protein kinase C β2	1700
Protein kinase C γ	500
Protein kinase C δ	1100
Protein kinase C ε	6500
Protein kinase C η	2000
Protein kinase C ζ	60,000
cAMP-dependent protein kinase	8000
cGMP-dependent protein kinase	1700
GSK3-β	10
ASK-γ (plant GSK-3)	80
Eg2 kinase	4000
CK1	35
CK2	7000
Insulin receptor tyrosine kinase	75,000
c-src tyrosine kinase	7000
c-abl tyrosine kinase	4000
Topoisomerase I	–(10,000)
Topoisomerase II α	–(10,000)

Enzyme activities were assayed as described in the Supplementary materials section, in the presence of increasing HD concentrations. IC_{50} values were calculated from the dose-response curves. –, no effect at the highest dose tested (in parentheses).

HD is a competitive inhibitor of ATP

To investigate the mechanism of HD action, kinetic experiments were performed by varying both ATP levels and HD concentrations (Figure 6a). Double-reciprocal plotting of the data demonstrates that HD is a competitive inhibitor for ATP. The apparent inhibition constant (K_i) was 50 nM. HD does not act by displacing cyclin B from CDK1 (Figure 6b).

Crystal structure of the CDK2–HD complex

Crystal structures of CDK2 complexed with several inhibitors have been reported: isopentenyladenine [41], olomoucine [41], des-chloro-flavopiridol [42], roscovitine [25], staurosporine [43], purvalanol [26] and indirubin-3′-monoxime [28]. All these compounds bind in the ATP-binding pocket located in the groove between the small and the large lobes of CDK2. To study in detail the essential binding interactions of HD, and to compare

Table 2

Inhibition of CDK1, CDK5 and GSK-3β and CK1 by HD analogues.

		IC_{50} (nM)			
	Compound	CDK1/cyclin B	CDK5/p25	GSK3-β	CK1
1	Hymenialdisine	22	28	10	35
	Hymenialdisine–platinum complex	30	200	130	1000
	Diacetylhymenialdisine	130	1500	160	550
	Diacetyldebromohymenialdisine	1300	3000	600	1100
4	Stevensine/odiline	70,000	– (100,000)	– (100,000)	– (100,000)
5	Axinohydantoin	4000	7000	3000	4500
8	Dibromophakellstatin	– (10,000)	– (100,000)	>10,000	– (10,000)
9	Agelastatin A	– (100,000)	– (100,000)	12,000	– (100,000)
10	Dibromocantharelline	>100,000	>100,000	3000	– (100,000)
11	Dispacamide A	– (100,000)	– (100,000)	– (100,000)	– (100,000)
12	Clathrodin	>100,000	>100,000	10,000	– (100,000)
13	Hymenidin	>100,000	4000	12,000	>100,000
14	Oroidin	>100,000	50,000	20,000	>100,000
15	Agelongine	– (100,000)	– (100,000)	– (100,000)	– (100,000)
6	Dibromoageliferin	>100,000	>100,000	11,000	– (100,000)
7	Sceptrin	– (100,000)	– (100,000)	– (100,000)	– (100,000)

Numbers refer to structures shown in Figure 1. Enzyme activities were assayed as described in the Supplementary material section, in the presence of increasing HD concentrations. IC_{50} values were calculated from the dose-response curves. –, no effect at the highest dose tested (in parentheses).

these with the interactions observed in the other CDK2–inhibitor complexes, we determined the structure of a CDK2–HD complex at 2.1 Å resolution (Table S1 in the Supplementary material section). Treatment with a cross-linking agent, prior to soaking, was necessary to prevent the crystal from cracking. The final model consists of 274 amino acid residues, one bound HD molecule, 85 solvent molecules and four molecules of ethylene glycol, with a crystallographic R-factor of 19.2% (R_{free} of 26.7%) and good geometry. Residues 36–44 and 149–163 of CDK2, which are part of two highly flexible loops, were left out from the final model because of weak or missing electron density. All nonglycine residues in the CDK2 model have mainchain torsion angles that lie well within

Figure 3

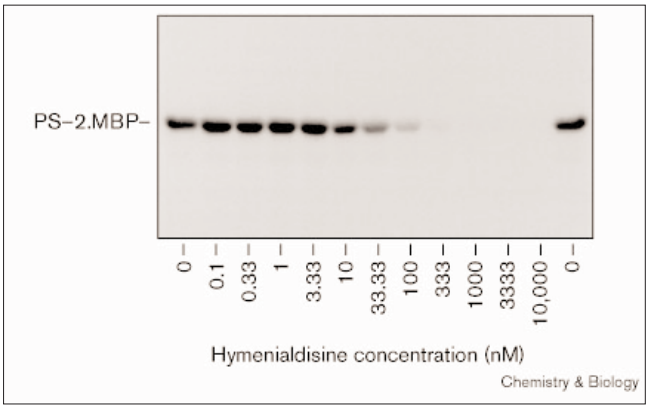

HD inhibits the phosphorylation of presenilin-2 by CK1 *in vitro*. A bacterially expressed fusion protein between presenilin-2 and maltose-binding protein (PS-2–MBP) was phosphorylated *in vitro* with CK1 in the presence of increasing HD concentrations and resolved by sodium dodecyl sulphate–polyacrylamide gel electrophoresis (SDS–PAGE), followed by autoradiography.

Figure 4

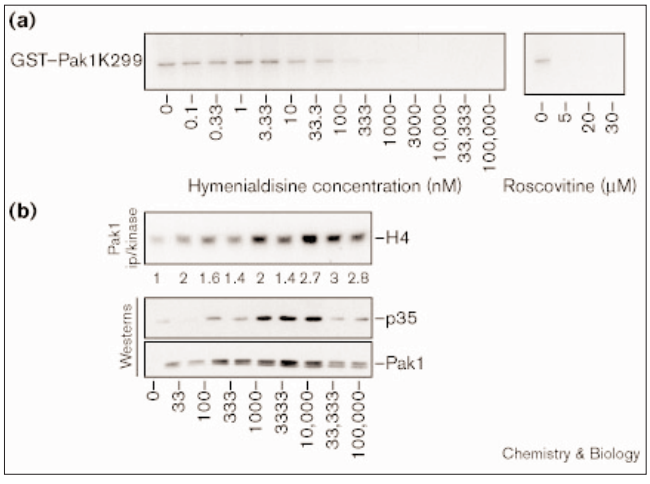

HD inhibits phosphorylation of Pak1 by CDK5/p35 *in vitro* and *in vivo*. Rat embryo cortical neurons were exposed to various HD concentrations for 1 h. Pak1 was then immunoprecipitated and its kinase activity towards histone H4 measured. **(a)** The level of H4 phosphorylation following SDS–PAGE of the substrate is shown. Numbers correspond to the quantification of the autoradiography. **(b)** Western blots show the amounts of Pak1 and p35. Note an increase in p35 levels as a consequence of CDK5 inhibition.

Figure 5

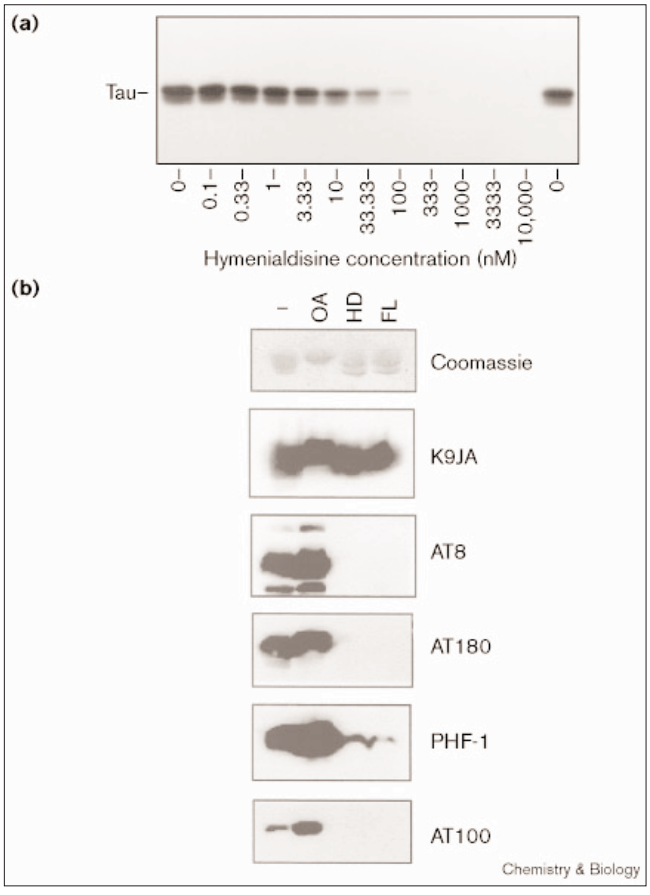

HD inhibits tau phosphorylation by GSK-3β *in vitro* and *in vivo*. **(a)** Bacterially expressed recombinant human tau was phosphorylated *in vitro* with GSK-3β in the presence of increasing HD concentrations and resolved by SDS–PAGE, followed by autoradiography. **(b)** Sf9 cells expressing htau23 were left untreated (–), or exposed to okadaic acid (OA), HD or flavopiridol (FL) for 5 h. Cell lysates (3 μg htau23) were resolved by SDS–PAGE, stained with Coomassie blue or immunoblotted with various antibodies: K9JA (a pan-tau antibody) recognizes all preparations that contain tau; AT8, AT180 and PHF1 are specific for different phosphorylated SP or TP motifs; AT100 recognizes tau phosphorylated at Thr212 and Ser214, a highly specific reaction for the Alzheimer's form of tau.

Figure 6

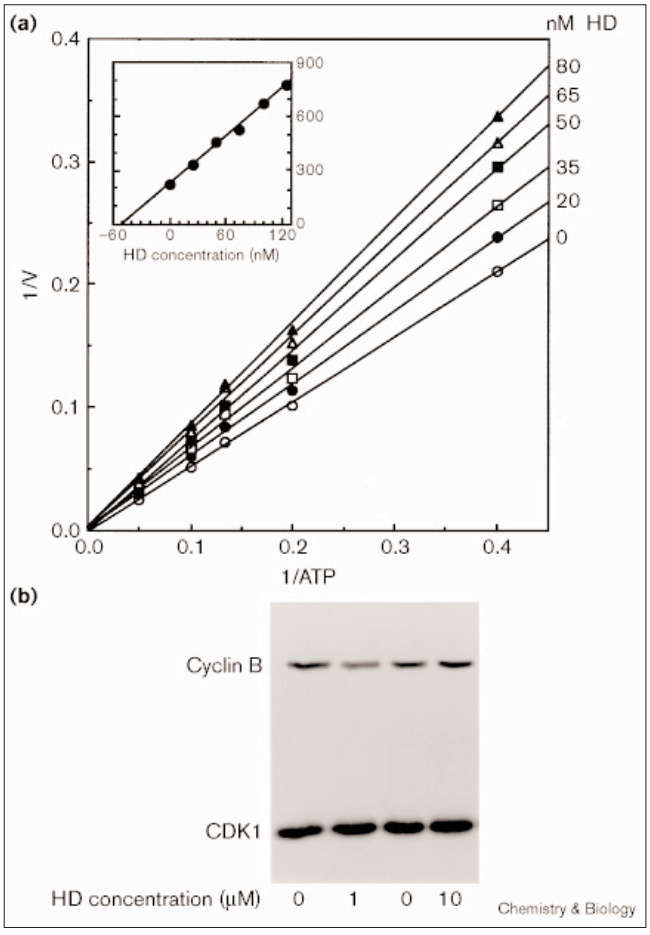

HD acts by competing with ATP. **(a)** Double reciprocal plots of kinetic data from assays of CDK1/cyclin B protein kinase activity at different concentrations of hymenialdisine. Enzyme activities were assayed as described in the Supplementary material section. **(a)** 1/V versus 1/ATP primary plot. ATP concentrations in the reaction mixture varied from 0.05 to 0.25 mM, concentration of histone H1 was kept constant at 0.7 mg/ml. Inset, secondary re-plots of slopes versus concentration from primary plots. The apparent inhibition constant (K_i) is indicated by an arrow. **(b)** HD does not release cyclin B from CDK1. p9CKShs1-sepharose-immobilised CDK1/cyclin B was exposed to HD for 30 min, washed and analysed by western blotting with anti-cyclin B and anti-PSTAIRE antibodies.

the energetically favorable regions of the Ramachandran plot [44], except for two residues, Glu73 and Arg126, that have backbone conformations falling just outside the 'additional allowed' region in ϕ–ψ space.

HD was unambiguously localised in a Fourier difference map, confirming that this inhibitor also binds in the ATP-binding pocket (Figure 7a). A representation of the binding-site interactions is shown in Figures 7b and 8. The pyrroloazepine double-ring system of HD fills a shallow hydrophobic pocket formed by Ile10, Val18, Ala31, Val64, Phe80 and Leu134, making several van der Waals contacts with the sidechain atoms of these residues. In addition, three hydrogen bonds are formed with the backbone of CDK2, between the N1 atom of the pyrrole ring and the carbonyl oxygen of Leu83, between the O1 carbonyl oxygen of azepine ring and the backbone amide of Leu83, and between the N2 amide of the azepine ring and the carbonyl oxygen of Glu81. The bromine atom bound to the pyrrolo ring of HD points towards the outside of the ATP-binding pocket, where it is partly exposed to solvent, but also packed against the mainchain carbonyl oxygen atoms of Ile10 and His84, and the sidechains of Ile10 and Leu134. Binding of the guanidine ring system of HD involves a few van der Waals contacts, mainly with the sidechain of Val18, in addition to one

Figure 7

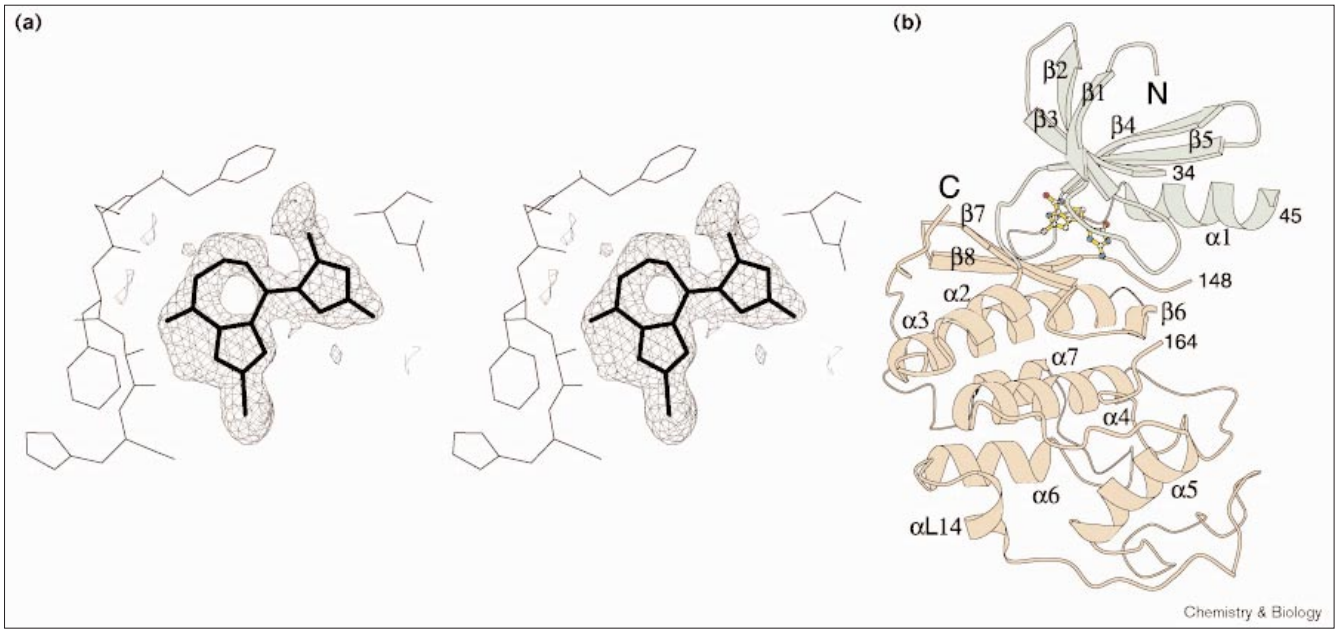

Overall structure of a CDK2–HD crystal. **(a)** Stereo view of the electron density for HD. The electron density at 2.1 Å resolution was drawn from a F_o–F_c difference omit electron density map calculated after simulated annealing refinement. The map was contoured at 2.0 σ. **(b)** Backbone drawing of CDK2 with HD in the ATP-binding pocket between the smaller amino-terminal domain and the larger carboxy-terminal domain. Secondary structural elements are indicated by arrows for β strands and coils for α helices, and labelled as in the apo-enzyme [74]. Drawn using MOLSCRIPT [75].

direct hydrogen bond between the N5 amino group of the guanidine and one of the sidechain oxygen atoms of Asp145, and two water-mediated hydrogen bonds between the O2 of HD and the mainchain NH of Asp145, and between the N5 of HD and the mainchain carbonyl of Gln131. Comparison with the apo-CDK2 and CDK2–ATP structures [45] reveals a large movement of Asp145 upon binding of HD, consisting of a 1 Å shift of the Cα atom, and a rotation of the sidechain of ~90° around the Cα–Cβ bond away from the HD guanidine ring. All the other residues in contact with the inhibitor have similar conformations to those observed in the apo-CDK2 and CDK2–ATP structures.

Comparison of CDK2–HD with other complexes

To provide a structural basis for understanding the potency of HD we compared the structure of the CDK2–HD complex with those of CDK2 complexed with ATP [45], staurosporine, flavopiridol and with the purine analogues olomoucine, roscovitine and purvalanol, as well as with the structure of the cyclin A–CDK2–ATP complex [46].

The hydrophobic double-ring system of HD binds at approximately the same position in CDK2 as the purine ring of ATP in the CDK2–ATP complex, similar to the positions of the double-ring systems in the other CDK2–inhibitor complexes (Figure 9). Although the orientation of the different double-ring systems varies significantly among the different inhibitors, it is restrained by the necessity to provide optimal shape complementarity with the shallow ATP-purine binding pocket while allowing the formation of a number of hydrogen bonds with the backbone of residues 81–83 at the cross-over connection in CDK2. The hydrogen-bonding interactions in the CDK2–HD complex seem to be the most favorable of all the CDK2–inhibitor complexes studied so far. The hydrogen bonds between N2 and the peptide oxygen of Glu81, and between O1 and the peptide amide of Leu83 resemble closely those between the adenine base of ATP and CDK2 and those in the complexes with staurosporine and flavopiridol. The third hydrogen bond in the CDK2–HD complex with the mainchain carbonyl of Leu83, is absent in these complexes, and can be observed only in the complexes with the three purine-based inhibitors olomoucine, roscovitine and purvalanol. Similar to HD, these latter three inhibitors also form three hydrogen bonds with the cross-over connection, but their interaction with the Glu81 peptide oxygen is much weaker, involving a rare C–H···O hydrogen bond with the acidic C8 atom of the purine ring [26].

The bromine atom of HD is bound close to a region in CDK2 that in the other CDK2–inhibitor complexes is occupied by a benzyl group. Binding of a hydrophobic group in this region, where it can pack against the sidechains of

Figure 8

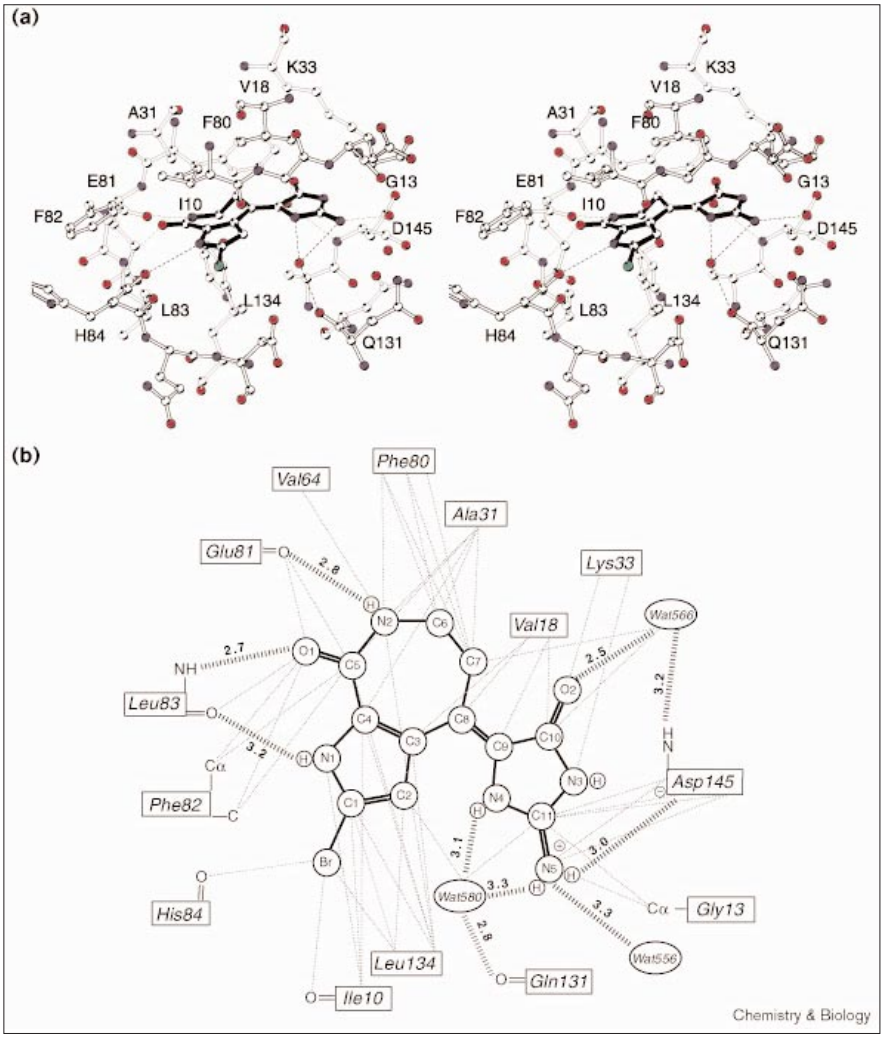

Protein–inhibitor interactions in the CDK2–HD complex. **(a)** Stereo diagram showing the refined structure of HD in the ATP-binding pocket of CDK2. Inferred hydrogen bonds are shown as thin dotted lines. Oxygen atoms are shown in red, nitrogen atoms in blue and bromine in green. **(b)** Schematic illustration of the interactions between CDK2 and HD. Protein sidechain contacts are indicated by lines connecting to the respective residue box, whereas interactions with mainchain atoms are shown as lines to the specific mainchain atom. Van der Waals contacts are indicated by dotted lines and hydrogen bonds by broken lines.

Ile10, Phe82 and the backbone of residues 82–84, is important for increasing the specificity of inhibitors for CDK2 [25,26,41]. Although the bromine in HD cannot provide the same number of interactions as a benzyl ring, the presence of this atom in HD probably contributes significantly to its binding affinity and specificity towards CDK2, as can been seen from the inhibitory activities of various HD analogues in Table 2 and Figure 2.

The region of CDK2 occupied by the guanidine ring of HD is also interesting. A superposition with the other CDK2–inhibitor complexes shows that only the flavopiridol and staurosporine inhibitors have groups bound in this region of CDK2, which partly overlaps with the pocket where the α-phosphate of ATP binds. Comparison of the structure of the CDK2–HD complex with that of the CDK2–flavopiridol complex [42] reveals a number of striking similarities between the binding modes of these structurally diverse inhibitors. The O2 carbonyl oxygen of HD is located close to the position of the O7 hydroxyl group of the flavopiridol, which emanates from the benzopyran ring bound at the purine region of the ATP-binding pocket. In both inhibitors the oxygen atoms form a water-mediated hydrogen bond with the mainchain amide of Asp145. Furthermore, the N5 amino group at the guanidine ring of HD is located near to the position of the positively charged amine group of the piperidinyl ring in the CDK2–flavopiridol complex. Both atoms are in hydrogen-bonding distance with the sidechain carboxylate of Asp145. The energetically favorable interaction between the positively charged amine group of the flavopiridol and the negatively charged carboxylate of Asp145 would make an important contribution to the binding strength of this inhibitor to CDK2. A similar interaction seems possible in the CDK2–HD complex, as under physiological conditions the guanidine ring is likely to be at least partly protonated at N3, thus providing a (partly) positive charge delocalised between N3, C11, N4 and N5 [33]. Also the

Figure 9

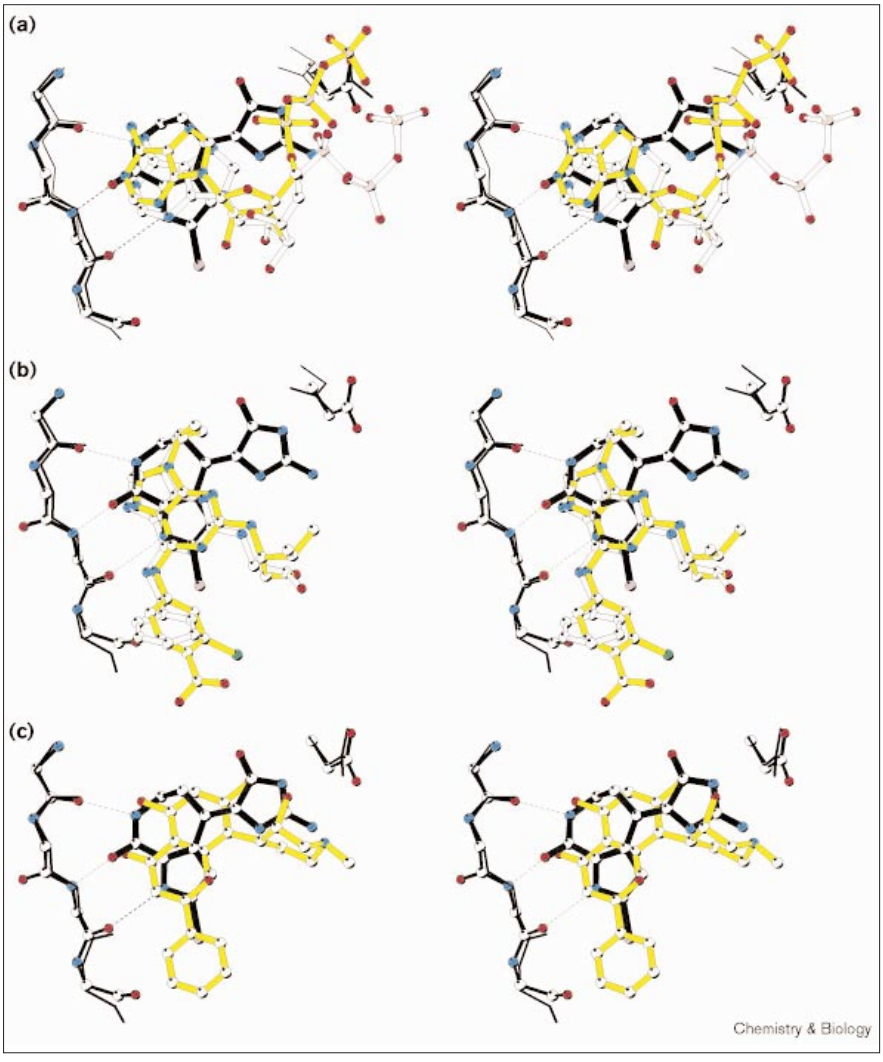

Stereo views comparing the binding of various CDK2 ligands or inhibitors. **(a)** Superposition of HD (black bonds) on ATP (white bonds) in apo-CDK2 and on ATP (yellow bonds) in the cyclin A–CDK2 complex. **(b)** Superposition of HD on olomoucine (white) and purvalanol (yellow). **(c)** Superposition of HD on flavopiridol. The CDK2 backbone atoms of residues 81–84, and the sidechain of Asp145 in the CDK2–HD complex are shown in ball-and-stick representation with black bonds. The same residues from the superimposed CDK2–ligand complex are shown as bonds. In (a) the thin bonds refer to the apo-enzyme, the thick bonds to the cyclin A–CDK2 dimers.

movement of Asp145 is conserved in both CDK2–inhibitor complexes. It is also seen in the indirubin-5-sulphonate–CDK2 structure [28]. Asp145 is part of the conserved Asp–Phe–Gly (DFG) motif found in most protein kinases [47]. Although significantly different from those in the CDK2–ATP complex, the position and conformation of Asp145 in both CDK2–inhibitor complexes is, in fact, very similar to those in the functionally more relevant cyclin A–CDK2–ATP complex [46] (Figure 9a).

In vitro inhibition of presenilin phosphorylation

We next investigated the effects of HD on the *in vitro* and *in vivo* phosphorylation of various protein substrates relevant to AD. The large hydrophilic loop of presenilin-2 between transmembrane domains 6 and 7 is a substrate for both CK1 and CK2 *in vitro*; this domain is phosphorylated *in vivo* [39]. Using a presenilin-2–maltose-binding protein (MBP) fusion protein as an *in vitro* substrate for CK1 we observed a dose-dependent inhibition of presenilin-2 phosphorylation by HD (Figure 3). MBP alone was not phosphorylated by CK1 (data not shown).

In vitro and *in vivo* inhibition of Pak1 phosphorylation by neuronal CDK5/p35

Among the physiological substrates of CDK5/p35 is the neuronal kinase Pak1 [18]. Both Pak1 and p35 associate with Rac, a small GTPase of the Rho family. Phosphorylation of Pak1 by CDK5/p35 results in inhibition of the Pak1 kinase activity [18]. Roscovitine inhibits CDK5/p35 and the resulting down-regulation of Pak1 both *in vitro* and *in vivo* [18]. These experiments were repeated with HD (Figure 4). First CDK5/p35 was immunoprecipitated from P02 rat cortices and its kinase activity towards GST–Pak1K299 (a kinase-dead Pak1 mutant) in the presence of HD, roscovitine or dimethylsulfoxide (DMSO) was assayed as described previously [18]. A dose-dependent

inhibition of CDK5 by HD was observed (IC_{50} values between 10 and 100 nM; Figure 4a). *In vivo* experiments were next performed using cultured neurons from E18 rat embryo cortices (Figure 4b). As previously shown [48], the amount of p35 increases with the extent of CDK5/p35 kinase inhibition. An increase in Pak1 activity was observed, consistent with an inhibition of endogenous CDK5 activity (Figure 4b).

HD inhibits MAP-1B phosphorylation by GSK-3 in cerebellar granule cell neurons

GSK-3β is inhibited by both WNT-7a and lithium in cerebellar granule cell neurons [49,50]. WNT-7a and lithium induce axonal remodelling and loss of a phosphorylated form of MAP-1B, a microtubule-associated protein involved in axonal outgrowth [50]. As GSK-3β phosphorylates MAP-1B at a site recognised by the antibody SMI-31, inhibition of GSK-3β by WNT or lithium results in the loss of a phosphorylated MAP-1B, MAP-1B-P [50]. To examine the effect of HD on neuronal morphology and MAP-1B phosphorylation cerebellar granule cells were cultured in different concentrations of HD. In control cells with long processes and very few filopodia (Figure 10a), MAP-1B-P is present along the entire length of the axon (Figure 10b). At low concentrations (1 μM, 10 μM and 25 μM) HD had no noticeable effect on the morphology of the cells (Figure 10c), or the distribution of MAP-1B-P (Figure 10d). However, 50 μM HD treatment induced axonal spreading and branching and a shortening of axon length (Figure 10e), with a concomitant loss of MAP-1B-P from most of the axonal processes (Figure 10f). Treatment of cultures with 100 μM HD caused a more dramatic change in cell morphology characterised by extensive branching and spreading, shortening of axon length and an increased number of filopodia (Figure 10g), together with loss of MAP-1B-P from processes (Figure 10h). The axonal remodelling observed was associated with a loss of stable microtubules from spread areas of the axons (data not shown). HD induces the loss of MAP-1B-P in a dose-dependent manner as determined by western blotting (Figure 10i). This effect is similar to that observed with lithium or WNT-7a treatment [50]. As we have shown that HD inhibits GSK-3β directly, our results suggest that the loss of MAP-1B-P and axonal remodelling induced by HD is a consequence of GSK-3β inhibition in cultured neurons.

Figure 10

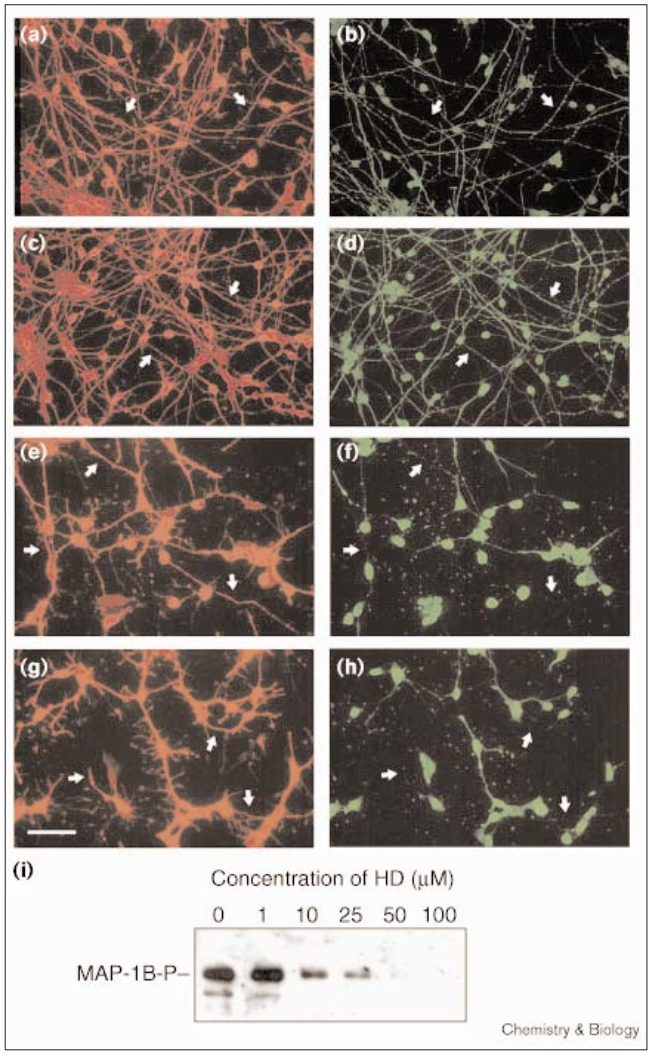

HD induces axonal remodelling and decreases GSK-3-induced MAP-1B-P levels in axonal processes. **(a**,**b)** Double immunofluorescence staining for GAP-43 (red) and MAP-1B-P (green) shows that MAP-1B-P is present along the axon. **(c)** A 20 h treatment with 10 μM HD has no obvious effect on cell morphology, or **(d)** MAP-1B-P localisation. Arrows indicate the same cells. **(e)** 50 μM HD treatment induces axonal spreading, shortening of the axon and **(f)** loss of MAP-1B-P from axonal processes. Arrows indicate the same cells. **(g)**100 μM HD treatment causes a more dramatic change in cell morphology with spreading and branching along the axon, an increased number of filopodia and shortening of the axon. **(h)** MAP-1B-P is lost from most of the axonal processes. Arrows indicate axons where MAP-1B-P is lost. Bar = 20 μm. **(i)** Western blotting analysis of cell lysates shows a gradual decrease in MAP-1B-P in response to increasing doses of HD.

Inhibition of tau phosphorylation by GSK-3

The microtubule-binding protein tau is the substrate of several kinases, including GSK-3β and CDK5/p35. Bacterially expressed recombinant human tau was indeed phosphorylated *in vitro* by GSK-3β and this phosphorylation was inhibited in a dose-dependent manner by HD, with an IC_{50} value of ~33 nM (Figure 5a). We next investigated the effect of HD on the *in vivo* phosphorylation of human tau23 expressed in Sf9 cells (Figure 5b). Cells were left untreated (–), or exposed to 0.2 μM okadaic acid (OA), 50 μM HD or 50 μM flavopiridol (FL), a CDK inhibitor that also inhibits GSK-3β (L.M., unpublished observations). Htau23 was resolved by using SDS–PAGE followed by immunoblotting with various antibodies. K9JA (a pan-tau antibody) recognizes all preparations that contain tau. AT8, AT180 and PHF1 are specific for different phosphorylated Ser–Pro (SP)

or Thr–Pro (TP) motifs: Ser202 and Thr205, Thr231 and Ser235, and Ser396 and Ser404, respectively, (as numbered in htau40, the longest human tau isoform). AT100 recognizes tau phosphorylated at Thr212 and Ser214; this reaction is highly specific for the Alzheimer's form of tau but occurs in Sf9 cells as well, provided both sites are phosphorylated [51]. The disappearance of AT100 signal following treatment with HD or flavopiridol indicates that both compounds are able to inhibit GSK-3β like activity in Sf9 cells.

Discussion

HD is a new and potent inhibitor of CDKs, GSK-3β and CK1. We have characterised its molecular interaction with CDK2, as well as its powerful effects on the *in vitro* and *in vivo* phosphorylation of neuronal proteins. Particularly interesting is the inhibitory effect of HD on the *in vivo* phosphorylation of the AD protein tau.

HD has been found in species of marine sponges belonging to the *Agelasidae*, *Axinellidae* and *Halichondriidae* families [33–36,52]. These animals contain a variety of substances that are clearly metabolically related to HD (e.g. Figure 1). The synthetic and degradation pathways of HD and how the related molecules fit in these pathways still remain to be investigated. Some experimental evidence suggests that oroidin and 4,5-dibromopyrrol-2-carboxylic acid, from *Agelas clathrodes*, act as 'feeding deterrent agents', protecting the sponge from predation by several species of fish [53].

Although HD inhibits CDKs by competition with ATP, it belongs to a new class of chemical CDK inhibitors. Previously described antagonists all act by competing with ATP binding. All interact with the ATP-binding pocket through two or three hydrogen bonds with the Glu81 and Leu83 residues of CDK2. The ATP-binding pocket of CDKs (and presumably of other kinases) can therefore accommodate an unexpectedly large variety of structures, with high affinity and high selectivity.

The potency of HD as a CDK inhibitor can be explained by analysing its binding interactions in the CDK2–HD crystal structure. Most of these interactions involve atoms of the HD pyrroloazepine ring system (which contribute 31 of the total 45 van der Waals contacts and three of the four direct hydrogen bonds). The van der Waals packing and hydrogen-bonding contacts of the HD double-ring system with the same, mostly hydrophobic enzyme residues that form the pocket for the adenine base in the ATP complex structure is a common feature in all crystallographically determined binding modes of CDK2 inhibitors, emphasising the anchoring nature of these interactions. Affinity and selectivity of the inhibitors is further built up from the binding of substituents that emanate from the double-ring system, which are different among the different inhibitors. One way to assess the binding strength of a ligand from its binding mode in a protein–ligand complex is the shape complementarity of the contact surfaces of both partners. These values are calculated from the structures of the different CDK2–inhibitor complexes (Table S2 in the Supplementary matieral section). For the three structurally related purine-based inhibitors, there is a good correlation between the inhibitory strength, and the shape complementarity with the inhibitor-binding pocket. For the structurally more diverse inhibitors des-chloro-flavopiridol and HD, however, shape complementarity alone seems to be a poor indicator of inhibitor strength. We believe that HD achieves tight binding to CDK2 through the contribution of strong specific hydrogen bonds, and a short-range electrostatic interaction between the acidic Asp145 and the basic guanidinium ring. In addition, a significant entropic factor could be involved in the binding of HD to CDK2, as the entropy penalty for the complex formation is minimal due to the rigid nature of the inhibitor. Nevertheless, one can imagine that drug-design studies could significantly improve the binding by optimising the shape complementarity of HD, for instance by replacing the bromine atom with more bulky groups. Unfortunately, at this point we are unable to identify the common structural features of the kinases for which HD is a potent inhibitor, nor explain why other kinases are not sensitive. Alignment of human CDK2, CK1 and GSK-3β (data not shown) is not especially helpful. Only the crystal structure of a CK1–HD or GSK-3β–HD will provide a clear view of the key interacting residues underlying the selectivity.

Investigating the selectivity of a compound is not a trivial matter. We feel that what is really important is the *in vivo* selectivity, the range of targets that an inhibitor will actually interact with within a cell. One method we are currently developing is the purification of targets using affinity chromatography on immobilised inhibitors. The crystal structure of the HD–CDK2 complex provides precious information with respect to its orientation within the ATP-binding pocket, showing which part of HD is accessible to solvent. This is where a linker could be attached to tether the inhibitor to a solid matrix while maintaining free access to its kinase targets. Using this approach with purvalanol, based on the CDK2–purvalanol crystal structure [26], we recently identified the intracellular targets of purvalanol in a variety of cells and tissues (Knockaert *et al.* and L.M., unpublished observations).

We are presently re-isolating HD-related compounds from marine sponges to investigate their CDK, GSK-3β and CK1 inhibitory properties. HD, the most abundant metabolite (up to 0.5% of the sponge dry weight), can also be used as a starting point for various chemical modifications, leading to new derivatives and this research is in progress in our laboratories. Furthermore, HD has been synthesised [54–56] and we are working on generating

new synthetic analogues. Finally, we have initiated a combinatorial chemistry approach to generate an even larger number of HD-related molecules. These various approaches, also partially guided by the CDK2–HD structure, should complement the initial structure–activity study presented in this paper. Through these various approaches, we hope to generate more selective and more cell-permeable HD analogues.

The kinases responsible for the hyperphosphorylation of tau and MAP-1B observed in AD certainly constitute reasonable screening targets. By acting on GSK-3β, CDK5 and CK1, the major kinases involved in this process, HD is a strong lead compound from which clinically useful drugs could potentially be generated. In addition to AD, HD could be used to target other neuronal disorders. For example, CDK5 is present in Lewy bodies, the typical inclusions observed in neurons in Parkinson's disease [57] and in glial cytoplasmic inclusions that characteristically occur in the oligodendrocytes of patients with multiple system atrophy [58]. CDK5 also accumulates in axonal swellings in dogs with hereditary canine spinal muscular atrophy [59]. Lithium is widely used for treatment of mood disorders, but its exact mechanism of action is not clearly defined. It appears to inhibit GSK-3β in a non-competitive way [60], thereby reducing tau phosphorylation [61–63]. The efficiency of HD towards GSK-3β (IC_{50} = 35 nM) compares very favourably with the relative efficacy of lithium towards GSK-3β (IC_{50} = mM).

Insulin acts by activating a protein kinase cascade leading to the inhibition of GSK-3β. This results in the stimulation of glycogen synthase and protein synthesis (reviewed in [64]). As a consequence, any GSK-3β inhibitor is a potential insulino-mimetic and could be useful in treating diabetes. This is certainly worth exploring with HD and its analogues.

Finally, it has been reported that HD inhibits NFκB activity through an alternate mechanism to inhibiting protein kinase C or IκB phosphorylation [65,66]. HD has also been reported to have anti-inflammatory properties [67]. The possibility that CDKs, GSK-3β, CK1, or another unknown kinase target of HD, are involved in NFκB activation and in adjuvant-induced arthritis deserves further investigation.

Significance

Among the estimated 2000 human protein kinases, cyclin-dependent kinase 5 (CDK5) and glycogen synthase kinase 3 (GSK3) appear to play an essential role in the hyperphosphorylation of substrates involved in Alzheimer's disease. While screening through a large collection of natural products derived from marine organisms, we identified hymenialdisine (HD) as a potent and rather selective inhibitor of these protein kinases. HD acts by competing with ATP for binding at the catalytic site of the kinase. HD was co-crystallised with CDK2, and the resolution of this complex structure provides data on the orientation and interactions of the inhibitor in the ATP-binding pocket of the kinase. It also allows some speculations on the further optimisation of HD analogues as kinase inhibitors. The *in vivo* effects of HD on kinases was demonstrated in several models. These results should encourage the study of HD as a lead compound in the treatment of neurodegenerative disorders.

Materials and methods

Preparation of CDK2–HD crystals

Human CDK2 was purified and crystallized as previously described [68]. Initial attempts to obtain CDK2–HD crystals, by adding small amounts of solid inhibitor to the crystal-containing drops, were unsuccessful because of insolubility of the inhibitor. When soaking with HD solubilized in the presence of 1% DMSO, however, it was observed that crystals cracked and dissolved at inhibitor concentrations as low as 10 μM, strongly suggesting that binding occurred (the same DMSO-containing solution without inhibitor did not harm the crystals). A procedure involving chemical cross-linking was employed to prevent crystals from cracking. Crystals were first soaked in a solution containing 0.5 mM ATP, 1 mM $MgCl_2$ for 2 h, then cross-linked with 0.1% glutaraldehyde, for 1 h at 4°C. After extensive washing the crystals were transferred to an inhibitor solution in 0.2 M HEPES, 5% ethylene glycol and 1% DMSO. This protocol allowed crystals to be soaked at inhibitor concentrations up to 0.5 mM, for several days, without showing any damage.

Determination of the CDK2–HD crystal structure

X-ray diffraction data to 2.1 Å resolution were collected on a single CDK2–HD crystal using an R-Axis II image plate detection system, mounted on a Rigaku rotation-anode generator. Data were collected at 120 K to prevent radiation damage of the crystal. Just prior to freezing, the crystal was transferred to a cryo-protecting solution containing 25% ethylene glycol. Flash freezing was achieved in a dry nitrogen stream using a Molecular Structure Corporation cryodevice. Freezing altered slightly the unit cell dimensions and increased the mosaic spread from 0.2–0.6°. The cross-linking by itself did not alter the diffraction characteristics significantly. The intensity data were processed with the DENZO and SCALEPACK programs [69]. The program TRUNCATE, as implemented in the CCP4 suite [70], was used to obtain the final set of structure factor amplitudes. A summary of the data processing statistics is presented in Table S1 in the Supplementary material section. Refinement of the CDK2–HD complex was started from the coordinates of the highly refined CDK2–ATP model. All refinement steps were carried out using the program X-PLOR [71]. Molecular replacement followed by rigid body refinement was necessary to successfully reorient and reposition the CDK2 molecule in the unit cell of the frozen crystal. The model was then further refined using several rounds of conjugated-gradient energy minimization. After this stage clear electron density, calculated from $2F_o–F_c$ and $F_o–F_c$ Fourier maps, indicated the binding mode of the hymenialdisine inhibitor. Initial coordinates and geometric restraint terms for hymenialdisine were taken from the small molecule structure of Mattia *et al.* [72]. Refinement of the CDK2–HD model was then pursued with several rounds of both X-ray restrained energy minimization and molecular dynamics, alternated with model building. Towards the end of the refinement several water molecules and a few molecules of ethylene glycol were added to the model. The stereochemistry of the CDK2–HD model was verified using the software package PROCHECK [73].

Accession numbers

The co-ordinates of the CDK2–hymenialdisine structure have been depostied in the PDB under the code 1DM2.

Supplementary material

Supplementary material including details of diffraction data collection and refinement statistics of the CDK2–HD complex, buried areas of CDK2 and ligands, chemicals and reagents used, buffers, kinase preparations and assays, electrophoresis and blotting, *in vitro* and *in vivo* phosphorylation of presenilin-2, Pak1, MAP-1B and tau and MAP-1B immunochemistry is available at http://current-biology.com/supmat/supmatin.htm.

Acknowledgements

We are grateful to the following people for providing reagents: F. Cafieri, M. Cobb, P. Davies, E. Fattorusso, M. Goedert, W. Harper, F. Hofmann, S. Lohmann, T.J. Lukas, H. Mett, M. Meyerson, A. Mangoni, L. Pinna, E. Sausville, O. Taglialatela-Scafati, H.Y.L. Tung, J.H. Wang, M. Watterson, G. Wilkin, J.R. Woodgett and M. Yamashita. We thank Dr A. Larsen for performing the topoisomerase I and II assays. We thank the fishermen of the 'Station Biologique de Roscoff' for collecting the starfish, J. Orillon for the photographic work and O. Collin for computer expertise. This research was supported by grants from the 'Association pour la Recherche sur le Cancer' (ARC 9314) (to L.M.) and the 'Conseil Régional de Bretagne' (to L.M.), Outstanding Investigator Grant CA-44344A1-05-10, U.S. National Cancer Institute, DHHS (to G.R.P.), the Arizona Disease Control Research Commission (to G.R.P.) and the Fannie E. Rippel Foundation (to G.R.P.). A.M.W.H.T. was supported by a long-term fellowship from the Human Frontier Science Program.

References

1. Selkoe, D.J. (1998). The cell biology of β-amyloid precursor protein and presenilin in Alzheimer's disease. *Trends Cell Biol.* **8**, 447-453.
2. Imahori, K., & Uchida, T. (1997). Physiology and pathology of tau protein kinases in relation to Alzheimer's disease. *J. Biochem.* **121**, 179-188.
3. Mandelkow, E.-M. & Mandelkow, E. (1998). Tau in Alzheimer's disease. *Trends Cell Biol.* **8**, 425-427.
4. Singh, T.J., Grundke-Iqbal, I. & Iqbal, K. (1995). Phosphorylation of tau protein by casein kinase 1 converts it to an abnormal Alzheimer-like state. *J. Neurochem.* **64**, 1420-1423.
5. Haas, C. & Mandelkow, E. (1999). Proteolysis by presenilins and the renaissance of tau. *Trends Cell Biol.* **9**, 241-244.
6. Anderton, B.H. (1999). Alzheimer's disease: clues from flies and worms. *Curr. Biol.* **9**, R106-R109.
7. Wolfe, M.S., Xia, W., Ostaszewski, B.L., Diehl, T.S., Kimberly, W.T. & Selkoe, D.J. (1999). Two transmembrane aspartates in presenilin-1 required for presenilin endoproteolysis and γ-secretase activity. *Nature* **398**, 513-517.
8. Yu, G., *et al.*, & Fraser, P.E. (1998). The presenilin 1 protein is a component of a high molecular weight intracellular complex that contains β-catenin. *J. Biol. Chem.* **273**, 16470-16475.
9. Zhang, Z.H., *et al.*, & Yankner, B.A. (1998). Destabilization of β-catenin by mutations in presenilin-1 potentiates neuronal apoptosis. *Nature* **395**, 698-702.
10. Takashima, A., *et al.*, & Wolzonin, B. (1998). Presenilin 1 associates with glycogen synthase kinase-3β and its substrate tau. *Proc. Natl Acad. Sci. USA* **95**, 9637-9641.
11. Takashima, A., *et al.*, & Yamaguchi, H. (1998). Activation of tau protein kinase I/glycogen synthase kinase-3β by amyloid β peptide (25–35) enhances phosphorylation of tau in hippocampal neurons. *Neurosci. Res.* **31**, 317-323.
12. Ebneth, A., *et al.*, & Mandelkow, E. (1998). Overexpression of tau protein inhibits kinesin-dependent trafficking of vesicles, mitochondria, and endoplasmic reticulum: implications for Alzheimer's disease. *J. Cell Biol.* **143**, 777-794.
13. Hudkins, R.L. (1999). ATP-site directed kinase inhibitors for therapeutic intervention. *Curr. Med. Chem.* **6**, 773-903.
14. Dunphy, W.G. (1997). *Methods in Enzymology: Cell-Cycle Control.* Academic Press, New York.
15. Morgan, D. (1997). Cyclin-dependent kinases: engines, clocks, and microprocessors. *Annu. Rev. Cell Dev. Biol.* **13**, 261-291.
16. Vogt, P.K. & Reed, S.I. (1998). *Current Topics in Microbiology and Immunology: Cyclin-Dependent Kinase (CDK) Inhibitors.* Springer Verlag, Berlin.
17. Garcia-Perez, J., Avila, J. & Diaz-Nido, J. (1998). Implications of cyclin-dependent kinases and glycogen synthase kinase 3 in the phosphorylation of microtubule-associated protein 1B in developing neuronal cells. *J. Neurosci. Res.* **52**, 445-452.
18. Nikolic, M., Chou, M.M., Lu, W., Mayer, B.J. & Tsai, L.-H. (1998). The p35/cdk5 kinase is a neuron-specific Rac effector that inhibits Pak1 activity. *Nature* **395**, 194-198.
19. Qi Z., Tang D.M., Zhu X.D., Fujita D.J., Wang J.H. (1998). Association of neurofilament proteins with neuronal Cdk5 activator. *J. Biol. Chem.* **273**, 2329-2335.
20. Meijer, L. & Kim, S.H. (1997). Chemical inhibitors of cyclin-dependent kinases. *Methods Enzymol.* **283**, 113-128.
21. Garrett, M.D. & Fattaey, A. (1999). CDK inhibition and cancer therapy. *Curr. Opin. Gene. Dev.* **9**, 104-111.
22. Gray, N.S., Détivaud, L., Doerig, C. & Meijer, L. (1999). ATP-site directed inhibitors of cyclin-dependent kinases. *Curr. Med. Chem.* **6**, 859-875.
23. Vesely, J., *et al.*, & Meijer, L. (1994). Inhibition of cyclin-dependent kinases by purine derivatives. *Eur. J. Biochem.* **224**, 771-786.
24. Meijer, L., *et al.*, & Moulinoux, J.P. (1997). Biochemical and cellular effects of roscovitine, a potent and selective inhibitor of the cyclin-dependent kinases cdc2, cdk2 and cdk5. *Eur. J. Biochem.* **243**, 527-536.
25. De Azevedo, W.F., Leclerc, S., Meijer, L., Havlicek, L., Strnad, M. & Kim, S.-H. (1997). Inhibition of cyclin-dependent kinases by purine analogues: crystal structure of human cdk2 complexed with roscovitine. *Eur. J. Biochem.* **243**, 518-526.
26. Gray, N.S., *et al.*, & Schultz P.G. (1998) Exploiting chemical libraries, structure, and genomics in the search for kinase inhibitors. *Science* **281**, 533-538.
27. Losiewiecz, M.D., Carlson, B.A., Kaur, G., Sausville, E.A. & Worland, P.J. (1994). Potent inhibition of cdc2 kinase activity by the flavonoid L86-8275. *Biochem. Biophys. Res. Commun.* **201**, 589-595.
28. Hoessel, R., *et al.*, & Meijer, L. (1999). Indirubin, the active constituent of a Chinese antileukaemia medicine, inhibits cyclin-dependent kinases. *Nat. Cell Biol.* **1**, 60-67.
29. Zaharevitz, D., *et al.*, & Sausville, E.A. (1999). Discovery and initial characterization of the paullones, a novel class of small-molecule inhibitors of cyclin-dependent kinases. *Cancer Res.* **59**, 2566-2569.
30. Schultz, C., *et al.*, & Kunick, C. (1999). The Paullones, a series of cyclin-dependent kinase inhibitors: synthesis, evaluation of CDK1/cyclin B inhibition, and *in vitro* antitumor activity. *J. Med. Chem.* **42**, 2909-2919.
31. Pettit, G.R., *et al.*, & Boyd, M.R. (1997). Antineoplastic agents. 362. Isolation and X-ray crystal structure of dibromophakellstatin from the Indian Ocean sponge *Phakellia mauritiana*. *J. Nat. Prod.* **60**, 180-183.
32. Pettit, G.R. (1996). Progress in the discovery of biosynthetic anticancer drugs. *J. Nat. Prod.* **59**, 812-821.
33. Sharma, G.M., Buyer, J. & Pomerantz, M.W. (1980). Characterization of a yellow compound isolated from the marine sponge *Phakellia flabellata*. *J. Chem. Soc. Chem. Commun.*, 435-436.
34. Cimino, G., de Rosa, S., de Stefano, S., Mazzarella, L., Puliti, R. & Sodano, G. (1982). Isolation and X-ray crystal structure of a novel bromo-compound from two marine sponges. *Tetrahedron Lett.* **23**, 767-768.
35. Kitagawa, I., Kobayashi, M., Kitanaka, K., Kido, M. & Kyogoku, Y. (1983). Marine natural products. XII. On the chemical constituents of the Okinawan marine sponge *Hymeniacidon aldis*. *Chem. Pharm. Bull.* **31**, 2321-2328.
36. Pettit, G.R., *et al.*, & Camou, F. (1990). Antineoplastic agents. 168. Isolation and structure of axinohydantoin. *Can. J. Chem.* **68**, 1621-1624.
37. Williams, D.H. & Faulkner, J. (1996). Isomers and tautomers of hymenialdisine and debromohymenialdisine. *Nat. Prod. Lett.* **9**, 57-64.
38. Carlson, B.A., Dubay, M.M., Sausville, E.A., Brizuela, L. & Worland, P.J. (1996). Flavopiridol induces G1 arrest with inhibition of cyclin-dependent kinase (CDK) 2 and CDK4 in human breast carcinoma cells. *Cancer Res.* **56**, 2973-2978.
39. Walter, J., Grünberg, J., Schindzielorz, A. & Haass, C. (1998). Proteolytic fragments of the Alzheimer's disease associated presenilins-1 and -2 are phosphorylated *in vivo* by distinct cellular mechanisms. *Biochemistry* **37**, 5961-5967.
40. Eldar-Finkelman, H. & Krebs, E.G. (1997). Phosphorylation of insulin receptor substrate 1 by glycogen synthase kinase 3 impairs insulin action. *Proc. Natl Acad. Sci. USA* **94**, 9660-9664.
41. Schulze-Gahmen, U., *et al.*, & Kim, S.-H. (1995). Multiple modes of ligand recognition: crystal structures of cyclin-dependent protein kinase 2 in complex with ATP and two inhibitors, olomoucine and

isopentenyladenine. *Proteins* **22**, 378-391.
42. De Azevedo, W.F., Mueller-Dieckmann, H.J., Schulze-Gahmen, U., Worland P.J., Sausville, E. & Kim, S.-H. (1996). Structural basis for specificity and potency of a flavonoid inhibitor of human CDK2, a cell cycle kinase. *Proc. Natl Acad. Sci. USA* **93**, 2735-2740.
43. Lawrie, A.M., Noble, M.E., Tunnah, P., Brown, N.R., Johnson, L.N. & Endicott, J.A. (1997). Protein kinase inhibition by staurosporine revealed in details of the molecular interaction with CDK2. *Nat. Struct. Biol.* **4**, 796-801.
44. Ramachandran, G.N., Ramakrishnan, C. & Sasisekharan, V. (1963). Stereochemistry of polypeptide chain configurations. *J. Mol. Biol.* **7**, 95-99.
45. Schulze-Gahmen, U., De Bondt, H.L. & Kim, S.-H. (1996). High-resolution crystal structures of human cyclin-dependent kinase 2 with and without ATP: bound waters and natural ligand as guides for inhibitor design. *J. Med. Chem.* **39**, 4540-4546.
46. Russo, A.A., Jeffrey, P.D. & Pavletich, N.P. (1996). Structural basis of cyclin-dependent kinase activation by phosphorylation. *Nat. Struct. Biol.* **3**, 696-700.
47. Hanks, S.K. & Hunter T. (1995). The eukaryotic protein kinase superfamily: kinase (catalytic) domain structure and classification. *FASEB J.* **9**, 576-96.
48. Patrick, G.N., Zhou, P., Kwon, Y.T., Howley, P.M. & Tsai, L.-H. (1998). p35, the neuronal activator of CDK5, is degraded by the ubiquitin-proteasome pathway. *J. Biol. Chem.* **273**, 24057-24064.
49. Lucas, F.R. & Salinas, P.C. (1997). WNT-7a induces axonal remodelling and increases synapsin I levels in cerebellar neurons. *Dev. Biol.* **193**, 31-44.
50. Lucas, F.R., Goold, R.G., Gordon-Weeks, P.R. & Salinas, P.C. (1998). inhibition of GSK-3β leading to the loss of phosphorylated MAP-1B is an early event in axonal remodelling induced by WNT-7a or lithium. *J. Cell Sci.* **111**, 1351-1361.
51. Zheng-Fischhöfer, Q., Biernat, J., Mandelkow, E.-M., Illenberger, S., Godemann, R. & Mandelkow, E. (1998). Sequential phosphorylation of tau-protein by GSK-3β and protein kinase A at Thr212 and Ser214 generates the Alzheimer-specific epitope of antibody AT-100 and requires a paired helical filament-like conformation. *Eur. J. Biochem.* **252**, 542-552.
52. Braekman, J.C., Daloze, D., Stoller, C. & Van Soest, R.W.M. (1992). Chemotaxonomy of *Agelas* (Porifera: Demospongiae). *Biochem. Syst. Ecol.* **20**, 417-431.
53. Chanas, B., Pawlik J.R., Lindel T. & Fenical W. (1996). Chemical defense of the carribean sponge *Agelas clathrodes* (Schmidt). *J. Exp. Mar. Biol. Ecol.* **208**, 185-196.
54. Annoura, H. & Tatsuoka T. (1995). Total syntheses of hymenialdisine and debromohymenialdisine: stereospecific construction of the 2-amino-4-oxo-2-imidazolin -5(Z)-disubstituted ylidene ring system. *Tetrahedron Lett.* **36**, 413-416.
55. Matsuki, S., Mizuno, A., Annoura, H. & Tatsuoka, T. (1997). Synthesis of pyrroloazepines. Facile synthesis of 2-substituted pyrrole derivatives by the phosgene method. *J. Heterocyclic Chem.* **34**, 87-91.
56. Xu, Y.Z., Yakushijin, K. & Horne, D.A. (1997). Synthesis of $C_{11}N_5$ marine sponge alkaloids: (±)-hymenin, stevensine, hymenialdisine, and debromohymenialdisine. *J. Org. Chem.* **62**, 456-464.
57. Brion, J.P. & Couk, A.M. (1995). Cortical & brainstem-type Lewy bodies are immunoreactive for the cyclin-dependent kinase 5. *Am. J. Pathol.* **147**, 1465-1476.
58. Nakamura, S., Kawamoto, Y., Nakano, S., Akiguchi, I. & Kimura, J. (1998). Cyclin-dependent kinase 5 and mitogen-activated protein kinase in glial cytoplasmic inclusions in multiple system atrophy. *J. Neuropathol. Exp. Neurol.* **57**, 690-698.
59. Green, S.L., Vulliet, P.R., Pinter, M.J. & Cork, L.C. (1998). Alterations in cyclin-dependent protein kinase 5 (CDK5) protein levels, activity and immunocytochemistry in canine motor neurone disease. *J. Neuropathol. Exp. Neurol.* **57**, 1070-1077.
60. Klein, P.S. & Melton, D.A. (1996). A molecular mechanism for the effect of lithium on development. *Proc. Natl Acad. Sci. USA* **93**, 8455-8459.
61. Hong, M., Chen, D.C., Klein, P.S. & Lee, V.M. (1997). Lithium reduces tau phosphorylation by inhibition of glycogen synthase kinase-3. *J. Biol. Chem.* **272**, 25326-25332.
62. Munoz-Montano, J.R., Moreno, F.J., Avila, J. & Diaz-Nido, J. (1997). Lithium inhibits Alzheimer's disease-like tau protein phosphorylation in neurons. *FEBS Lett.* **411**, 183-188.
63. Lovestone, S., *et al.*, & Anderton, B.H. (1999). Lithium reduces tau phosphorylation: effects in living cells and in neurons at therapeutic concentrations. *Biol. Psychiatry* **45**, 995-1003.
64. Cohen, P. (1999). The Croonian lecture 1998. Identification of a protein kinase cascade of major importance in insulin signal transduction. *Phil. Trans. R. Soc. Lond. B* **354**, 485-495.
65. Breton, J.J. & Chabot-Fletcher, M.C. (1997). The natural product hymenialdisine inhibits interleukin-8 production in U937 cells by inhibition of nuclear factor-B. *J. Pharmacol. Exp. Therap.* **282**, 459-466.
66. Roshak, A., Jackson, J.R., Chabot-Fletcher, M. & Marshall L.A. (1997). Inhibition of NFκB-mediated interleukin-1b-stimulated prostaglandin E2 formation by the marine natural product hymenialdisine. *J. Pharmacol. Exp. Therap.* **283**, 955-96.
67. Di Martino, M., Wolff, C., Patil, A. & Nambi, P. (1995). Effects of a protein kinase C inhibitor (PKCI) on the development of adjuvant-induced arthritis (AA) in rats. *Inflamm. Res.* **2**, S123-S124.
68. Rosenblatt, J., De Bondt, H.L., Jancarik, J., Morgan, D.O. & Kim, S.-H. (1993). Crystal structure of cyclin-dependent kinase 2. Purification and crystallization of human cyclin-dependent kinase 2. *J. Mol. Biol.* **230**, 1317-1319.
69. Otwinowski, Z. & Minor, W. (1997). Processing of X-ray diffraction data collected in oscillation mode. *Methods Enzymol.* **276**, 307-326.
70. Collaborative Computational Project, Number 4. The CCP4 suite: programs for protein crystallography. *Acta Crystallogr. D* **50**, 760-763.
71. Brünger, A.T. (1993). *X-PLOR, Version 3.1. A System for Protein Crystallography and NMR*. Yale University Press, New Haven, CT.
72. Mattia, C.A., Mazzarella, L. & Puliti, R. (1982). 4-(2-amino-4-oxo-2-imidazolin-5-ylidene)-2-bromo-4,5,6,7-tetrahydropyrrolo-[2,3-c]azepin-8-one methanol solvate: a new bromo compound from the sponge *Acanthella aurantiaca*. *Acta Crystallogr. B* **38**, 2513-2515.
73. Laskowski, R.A., MacArthur, M.W., Moss, D.S. & Thornton, J.M. (1993). PROCHECK: a program to check the stereochemical quality of protein structures. *J. Appl. Crystallogr.* **26**, 283-291.
74. De Bondt, H.L., Rosenblatt, J., Jancarik, J., Jones, H.D., Morgan, D.O. & Kim, S.H. (1993). Crystal structure of cyclin-dependent kinase 2. *Nature* **363**, 595-602.
75. Kraulis, P.J. (1991). MOLSCRIPT: a program to produce both detailed and schematic plots of protein structures. *J. Appl. Crystallogr.* **24**, 946-950.

Because *Chemistry & Biology* operates a 'Continuous Publication System' for Research Papers, this paper has been published via the internet before being printed. The paper can be accessed from http://biomednet.com/cbiology/cmb – for further information, see the explanation on the contents pages.